Steady and Unsteady Computational Results of Full Two Dimensional Governing Equations for Annular Internal Condensing Flows

R. Naik*, S. Mitra, A. Narain and N. Shankar
Michigan Technological University
*Houghton, MI, USA. Email: rrnaik@mtu.edu

Abstract: This paper presents steady and unsteady computational results obtained from numerical solutions of the full two-dimensional governing equations for annular internal condensing flows in a channel. These are achieved by implementing the MATLAB codes (developed for this algorithm) with COMSOL's fluid flow and heat transfer modules. This technique allows for an accurate wave simulation technique for the highly sensitive, shear-driven, annular condensing flows.

The unsteady wave simulation capability is used to predict heat-transfer rates and lengths of the annular regime for condensing flows. In other words, the technique can identify the transition of a shear-driven steady flow from the annular regime to other non-annular regimes. In addition, results obtained for inclined, horizontal, and zero-gravity cases bring out the differences between shear driven and gravity assisted/driven flows. This accurate simulation capability leads to significant improvements over our earlier reported simulation capabilities and over other existing fixed grid solution techniques.

Keywords: Phase-change, internal condensing flows

1. Introduction

Effective operation of boilers and condensers need stable, repeatable, and predictable realizations of annular boiling and condensing flows. New innovative devices of mm-scale hydraulic diameters have been shown to operate under only annular regimes ([1]). These high heat-transfer devices are being developed for space-based thermal management systems, power generation, electronic/data-center cooling applications, etc.

Space based and/or miniaturized operations pose many severe challenges. These include - smaller annular regimes (Fig. 1), problems with bubble detachment within boilers, and extreme sensitivity to ever-present noise/fluctuations. Accurate prediction of these flows is essential for effective design of condensers and boilers.

The typical traditional operation of ground-based gravity driven/assisted systems of larger hydraulic diameter (> 5 mm) are effective due to the presence of longer annular regimes (Fig. 1) which have higher thermal and hydrodynamic efficiency relative to non-annular regimes.

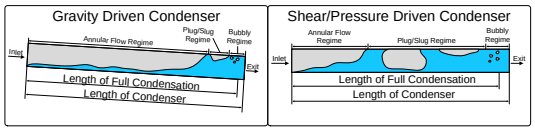

Figure 1. Schematic of gravity driven and shear/pressure driven condenser

This paper presents steady and unsteady computational results obtained from numerical solutions of the full two-dimensional governing equations for annular internal condensing flows in a channel. The computational methodology presented is, in essence, similar to our earlier methodology employed on the FORTRAN platform. The methodology has been well tested and validated by comparison with condensing flow experiments ([2-5]]). However, these earlier implementations were all for unsteady gravity driven flows. The algorithm reported here are the only ones which are for both gravity and shear driven condensing flows.

This paper presents the governing equations, computational approach and the solution algorithm utilized to develop the unsteady computational tool on the COMSOL/MATLAB platform. This tool is based on an approach ([6]) that models interface as a "sharp curve" between the liquid and vapor. Separate CFD calculations for each of the two phases are done on COMSOL. An iterative improvement and assembly of the separate single-phase solutions is then accomplished in conjunction with the interface tracking. This accurate interface tracking is done on a separate moving grid with the help of our own subroutines on MATLAB. For unsteady interface tracking, a new and improved approach of locating the interface by a suitable combination of explicit and implicit methods has been used. The steady-state computational tool and algorithm has been explained in [7, 8].

The proposed approach is different from the approach of other level-set and VOF techniques [9-13] on three counts: (i) the "interface" is

modeled as "sharp" instead of the more common "thin zone" models, (ii) the liquid and vapor domains are solved separately and consecutively as opposed to the concurrent solving of both domains, and (iii) the original hyperbolic nature of the interface tracking equation is retained without tweaking it with diffusive terms for computational convenience (see [14]) or as an ad-hoc improvements in some of the VOF techniques within the "thin zone" model.

The paper compares and finds good agreement of the reported steady results with the results obtained from two independent computational techniques, namely: the two-dimensional (2-D) technique implemented on FORTRAN [6] and a quasi one-dimensional technique [15]. The 2-D technique on FORTRAN utilizes a similar computational methodology outlined in this paper, but has greater limitations compared to the COMSOL based tool. The present tool allows for the handling of a larger domain size by integration of multiple domain solutions, and offers enhanced computational speed, higher accuracy, etc. The 1-D technique ([15]) is used for computing approximate results based on an algorithm that solves the governing equations as a set of non-linear ordinary differential equations.

The reported steady/unsteady computational methodology allows for the investigation of annular/stratified condensing flows, study of the steady flow's response to disturbances and sustained inlet mass flow rate pulsations, and prediction of the annular regime length. These issues are particularly important in understanding flow physics and the boundary condition sensitivity of shear driven flows typically realized in horizontal channel flows, micro-gravity flows and in micro-meter scale hydraulic diameter ducts.

2. Governing Equations

The two-dimensional computational approach employed to investigate internal condensing flows in channels and tubes is based on the full governing equations described in [6].

The liquid and vapor phases in the flow (see schematic in Fig. 2) are denoted with subscript I = 1 (alternatively as 'L') and I = 2 (alternatively as 'V') respectively. The fluid properties (density ρ, viscosity μ, specific heat C_p, and thermal conductivity k) with subscript I are to take their representative constant values for each phase (I = 1 or 2).

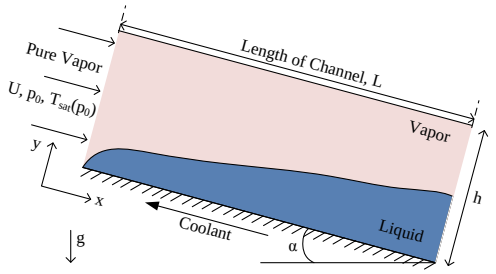

Figure 2: A schematic of a representative condensing flow problem in a channel.

Let T_I be the temperature fields, p_I be the pressure fields, and $\vec{v}_I = u_I\hat{i}+v_I\hat{j}$ be the velocity fields. Also, let $T_{sat}(p)$ be the saturation temperature of the vapor as a function of local pressure p at the interface, δ be the film thickness, $\dot{m}$ be the local interfacial mass flux, $T_w(x) < T_s(p)$ be a known temperature variation of the condensing surface (with its length-averaged mean value being $\overline{T}_W$).

Let g_x and g_y be the components of gravity along the x and y axes, p_0 be the steady inlet pressure, $\Delta T \equiv T_s(p_0) - \overline{T}_W$ be a representative controlling temperature difference between the vapor and the bottom plate, h_{fg} be the heat of vaporization at temperature T_s (p), and U be the average inlet vapor speed determined by the inlet mass flow rate $\dot{M}_{in}$ ($\equiv \rho_2 \bullet U \bullet h$ for the channel flow).

2.1 Interior Equations

The differential forms of mass, momentum (x and y components), and energy equations for 2-D flow in the interior of both the incompressible phases are the well-known equations (as in Eq. 2 in [6]).

2.2 Interface Conditions

The nearly-exact interface conditions for condensing flows are given in [6] and [16]. Utilizing a superscript "i" for values of flow variables at the interface $\emptyset \equiv y - \delta(x,t)=0$, non-dimensional forms of the interface conditions are given below.

The interfacial conditions are as follows:

- Continuity of liquid and vapor tangential component of interfacial velocities yields ([6]):

$$u_2^i = u_1^i - \delta_x (v_2^i - v_1^i), \qquad (1)$$

where $\delta_x \equiv \partial\delta/\partial x$.

• Normal component of momentum balance at the interface yields ([6]):

$$\pi_1^i = \frac{\rho_2}{\rho_1}\pi_2^i - \frac{1}{We}\left(\frac{\delta_{xx}}{[1+\delta_x^2]^{3/2}}\right) + \dot{m}^2\left(\frac{\rho_1}{\rho_2} - 1\right), \quad (2)$$

where $We \equiv \rho_1 U^2 h/\sigma$, and surface tension $\sigma = \sigma(T)$ where T is the interfacial temperature.

• Tangential component of momentum balance at the interface yields ([6]):

$$\frac{\partial u_1}{\partial y}\Big|^i = \frac{\mu_2}{\mu_1}\frac{\partial u_2}{\partial y}\Big|^i + [t], \quad (3)$$

where the term [t] is defined in Eq. (A.9) of [6].

• Non-zero interfacial mass fluxes $\dot{m}_{LK}$ and $\dot{m}_{VK}$ are obtained from kinematic constraints on the interfacial values of the liquid and vapor velocity fields and these are given by Eq 6 in [6].

• Non-zero interfacial mass flux $\dot{m}_{Energy}$ (as given by Eq. 7 of [6]) represents the constraint imposed by net heat flux (associated with latent heat release) across the interface.

• The interfacial mass balance requires that the net mass flux (in $kg/m^2/s$) at a point on the interface be single-valued regardless of which physical process is used to obtain it. This requirement essentially implies:

$$\dot{m}_{LK} = \dot{m}_{VK} = \dot{m}_{Energy} \equiv \dot{m}. \quad (4)$$

For the reported results, it should be noted that negligible interfacial thermal resistance and equilibrium thermodynamics is assumed to hold on either side of the interface for all points downstream of the origin.

•The non-dimensional form of the thermodynamic restriction on interfacial temperatures yields:

$$\theta_1^i \cong \theta_2^i = T_s(p_2^i)/\Delta T \equiv \theta_S(\pi_2^i) \quad (5)$$

Within the vapor phase, for the mm-scale ducts and refrigerants considered here, changes in absolute pressure relative to the inlet pressure are large enough to affect vapor motion but, at the same time, are too small (except in micro-scale ducts) to affect saturation temperatures. Therefore, we have $\theta_S(\pi_2^i) \cong \theta_S(0)$.

2.3 Boundary Conditions

The problem is computationally solved subject to the boundary conditions shown on a representative film profile in Fig 3.

Top wall: The upper wall temperature $T_2(x, h, t) > T_{sat}(p_0)$ is at a superheated value close to saturation temperature to allow the assumption of a nearly constant saturation temperature for the vapor at all location. This is reasonable because the effects of superheat (typically in a range of 5 – 10°C) are negligible.

Bottom wall: Besides the no-slip condition ($u_1(x, 0, t) = v_1(x, 0, t) = 0$) at the condensing surface, condensing-surface temperature ($T_1(x, 0, t) = T_w(x)$).

Inlet Conditions: At the inlet x = 0, we have $u_2 = U$, the prescribed inlet velocity.

Pressure is not prescribed across the inlet boundary but its value p_{exit} is specified at the corner point at the intersection of the inlet and the top wall. The inlet pressure p_{in} (= p_0) appears indirectly through important thermodynamic properties such as $h_{fg}(p_2^i) \approx h_{fg}(p_0)$ and $T_{sat}(p_2^i) \approx T_{sat}(p_0)$. Interfacial pressure variations are obtained from the computed non-dimensional pressures $\pi_2^i(x, y, t)$ through the relation $p_2 = p_0 + \rho_2.U^2\,\pi_2(x, \delta(x, t), t)$.

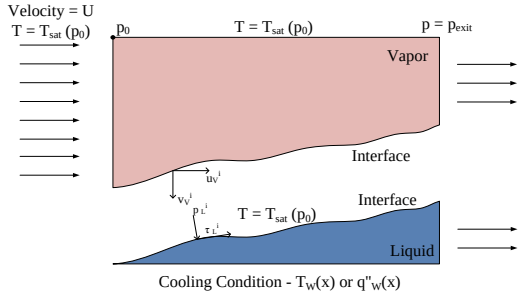

Figure 3: For a representative film profile the figure shows the boundary conditions for the liquid and vapor domain.

3. Computational Approach

The computational approach consists of two parts - the steady solution approach and the unsteady solution approach.

For the steady solution approach, though not necessary, a sophisticated quasi one-dimensional model ([15]) is used to provide initial guesses of interface location and interfacial velocity of the steady, annular/stratified flow in this geometry. This choice expedites convergence. Subsequently, starting from this guess, the new computational tool based on COMSOL and MATLAB subroutines is used to improve the interface location and to solve condensing flow problems. The approach is similar to ([1]-[7]) that uses as a sharp interface model and performs separate CFD calculations for each one of the two phases. Continuous improvements by the iterative assembly of the two separate single-

phase solutions in conjunction with interface tracking with the help of our own subroutines on MATLAB leads to convergence and accurate solution. The simulation tool locates an interface ($\phi(x, y, t) = 0$) by solving the interface tracking equation arising from one of the interfacial mass-flux condition as in Eq. (4):

$$\dot{m}_{LK} = \dot{m}_{Energy} \quad (6)$$

This requirement is rewritten in the popular interface evolution equation form:

$$\frac{\partial \emptyset}{\partial t} + \vec{V}_{eff}.\vec{\nabla}\emptyset = 0 \quad (7)$$

where $\vec{V}_{eff} = \vec{v}_1^{\,i} - \left(k_1.\vec{\nabla}T_1|^i - k_2.\vec{\nabla}T_2|^i\right).(1/\rho_1).(1/h_{fg})$ is the modified velocity vector determined by the vertical component of liquid interfacial velocity $\vec{v}_1^{\,i}$ and liquid and vapor temperature gradients at the interface ($\vec{\nabla}T_1|^i$ and $\vec{\nabla}T_2|^i$).

The above equation is currently solved by a 2D interface tracking method valid only for an explicit definition of ϕ given as: $y - \delta(x,t) = 0$ for the unsteady case and $y - \delta_{Steady}(x,t) = 0$ for the steady case. In a forthcoming approach, we will propose an enhancement of this interface tracking method by a level-set type technique [12] without the assumption on the form of ϕ.

3.1 Interface Tracking

The interface is tracked as by solving a reduced form of Eq. 6. This reduced form is given by:

$$\frac{\partial \delta}{\partial t} + \bar{u}(x,t)\frac{\partial \delta}{\partial x} = \bar{v}(x,t) \quad (8)$$

where $\delta(x, 0) = \delta_{Steady}$ or other prescriptions, $\bar{u}(x,t)$ and $\bar{v}(x,t)$ definitions can be found in [6].

This interface evolution equation is a wave equation, which is a first order hyperbolic partial differential equation (PDE). Its characteristics, characteristic speeds, and forcing functions can be determined by marching forward in time. This evolution equation is solved with 4th order accuracy in time using its well-defined characteristics equation (which is an ODE underlying the PDE problem).

The solution of Eq. 8 (evolution of the interface) is observed along the characteristic curves $x = x_c(t)$ given by

$$\frac{dx_c}{dt} = \bar{u}(x_c(t), t) \quad (9)$$

Eq. 9 is solved by a 4th order Runge-Kutta method (RK4) to obtain $x_c(t)$ curves for $t \geq 0$ under initial conditions $x_c(0) = x^*$ where x^* is any value between inlet and outlet. For $x_c(t)$ curves starting at $x = 0$, Eq. 9 is solved over $t \geq t^*$ where t is any specific time and $x_c(t^*) = 0$.

The evolution of the film along the characteristic curves is governed by

$$\frac{d\hat{\delta}(t)}{dt} = \hat{\bar{v}}(x_c(t), t) \quad (10)$$

$$\hat{\delta}(0) = \delta_{Steady} \text{ or other prescriptions}$$

where $\hat{\delta}(t) = \delta(x_c(t), t)$ and $\hat{\bar{v}}(t) = \bar{v}(x_c(t), t)$.

Interface evolution equation is solved by using a mix of explicit and implicit tracking approaches. The interface at time, $t = t^* + \Delta t$, is predicted explicitly along the characteristic curves (use Eq. 24 in [6]). The single-phase domain solutions are then recomputed. The recomputed single-phase domain solutions, along the previous prediction of film is used to further refine the prediction of film at $t = t^* + \Delta t$. This is accomplished by the utilizing 4th order RK4 method for Eqns. 9 - 10. This algorithm leads to accurate satisfaction of the interface conditions (including the interfacial mass flux conditions).

4. Solution Algorithm

The solution algorithm is as follows:

i) At discrete number of spatial locations, an initial guess of interface variables - δ, τ^i, p^i, $T_L{}^i$, $u_V{}^i$, $v_V{}^i$, $T_V{}^i$ for the steady problem are made. For the unsteady problem, the algorithm starts with known or specified values of these variables at $t = 0$.

ii) Liquid domain is solved on COMSOL using the **Laminar Flow** model under the **Single-Phase Flow** branch and the **Heat Transfer in Fluids** model, using stress boundary conditions - i.e. tangential stress (shear) and normal stress (pressure) specified, and using saturation temperature conditions at the interface. The converged solution is post-processed on MATLAB to obtain $u_L{}^i$, $v_L{}^i$, $T_L{}^i$.

iii) Using the liquid domain solution, $u_V{}^i$ and $v_V{}^i$ are obtained from continuity of tangential velocity and interfacial mass flux equality respectively. $T_V{}^i$ is obtained from saturation temperature conditions at the interface.

iv) Using the values of $u_V{}^i$, $v_V{}^i$, $T_V{}^i$ on the current location of the interface δ, the vapor domain is solved on COMSOL using the **Laminar Flow** model (but Turbulence Flow model can also be used far away from the interface) under the **Single-Phase Flow** branch. The solution is post-

processed to obtain values of tangential and normal stresses at the vapor interface.

v) The momentum-balance condition at the interface and the computed values of vapor domain interfacial stresses are used together to obtain the new updated values of interfacial stresses at the liquid domain interface.

vi) The initial values for the interface location ($\delta(x, t) = 0$) at $t = t^*$ predict the interface location at discrete values of $t = t^* + \Delta t$ and on a moving grid x. With his new predicted interface location, steps (i) - (v) are repeated until a good estimate of the interface location at $t = t^* + \Delta t$ is obtained. Combinations of explicit and implicit methods are used for the interface tracking. This also ensures that the effective velocity $\vec{V}_{eff}$ used in the interface tracking equation is converged.

Repetition of the steps (i) to (vi) yields converged interface locations as well as CFD solutions for liquid and vapor domains at each $t = n\Delta t$ for n = 1, 2, etc.

5. Results and Discussion

5.1 Convergence of the solution

Accuracy (shown in [8]) of the solution is ensured by the following:

i. The convergence of flow variables in the interior of each single-phase fluid domain.
ii. Satisfaction of all the interface conditions for the condensing flow problem.
iii. Grid independence of each single-phase domain and convergence of the flow variables.

5.2 Ability of the tool to satisfy steady/unsteady interface conditions

The ability to satisfy the interface conditions is an extremely critical aspect of simulations for free-surface problems. The existing VOF and Level-set techniques, due to their use of a band approach to track the interface, are typically unable to accurately satisfy the independent verification of the interfacial mass fluxes of Eq. 4 (as shown in the schematic of Fig. 4). However, in this approach, the mass fluxes based on liquid kinematics ($\dot{m}_{LK}$), vapor kinematics ($\dot{m}_{VK}$), and energy constraints ($\dot{m}_{Energy}$) are found, in Fig. 5, to be in very good agreement with one another.

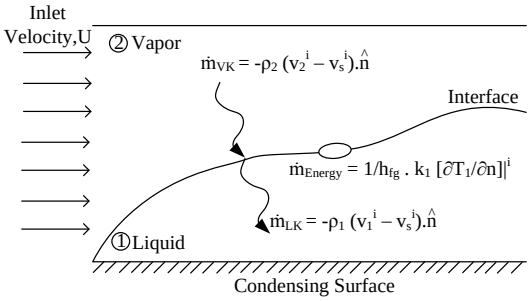

Figure 4. Schematic of a condensing flow showing the method of computing the interfacial mass fluxes (kg/m^2-s) based on liquid kinematics ($\dot{m}_{LK}$), vapor kinematics ($\dot{m}_{VK}$), and energy constraints ($\dot{m}_{Energy}$)

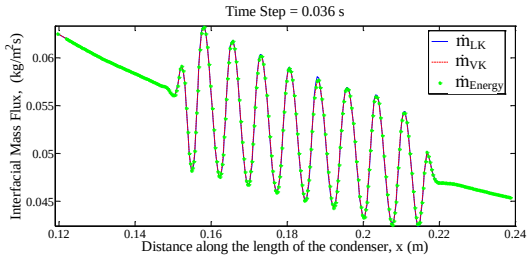

Figure 5. Interfacial mass fluxes (kg/m^2-s) at a specific time instant during an unsteady simulation showing very good agreement.

5.3 Features of steady solution

The steady solution obtained from the current simulation technique has also shown to be in agreement with both the 1-D Engineering technique [8] and the previous 2-D Fortran tool [17]. Fig. 6 shows the comparison of the non-dimensional film thickness values along the length of the channel from three different simulation techniques.

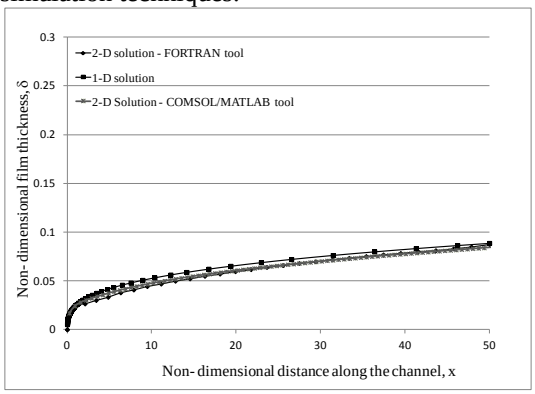

Figure 6. Comparison of non-dimensional film thickness along the non-dimensional length of the channel from the current 2-D steady tool, 1-D technique [10], and the 2-D steady Fortran tool showing good agreement.

Table 1 shows the comparison of the simulation heat-flux with the experimental results for run cases of [18]. The experimental inlet mass flow rates and boundary conditions (particularly of spatially varying wall temperatures) have been used for the simulations. The table shows good agreement for heat-flux values measured experimentally at a 40 cm location from the inlet of the test section. This shows the ability of the code to handle different non-uniform and realistic boundary conditions of real world condenser situations. Prescribed heat-flux thermal boundary conditions can also be used with minor changes to the code.

Figure 7 shows the streamline patterns for a shear-driven flow and a gravity assisted (inclined channel of 2 deg) flow indicating the tendency of the film to fly-off from the surface in the absence of a gravitational component in the direction of the flow. This is an indication of an earlier transition to non-annular regimes for the shear-driven flow and hence a shorter annular regime length (x_A) in comparison to the gravity assisted situation. With the help of this understanding, our research team has proposed ([1]) innovative operations of such condensers and boilers.

Table 1. Comparison of steady 2-D simulation results with experimental run cases in [18]

Case	$\overline{\dot{M}}_{in}$	$T_{sat}(\overline{p}_{in})$	$\overline{T}_W$	$\overline{q''}_{W\|Expt}$ @ x = 40	$\overline{q''}_{W\|2\text{-}D}$ @ x = 40 cm	% Error for 2-D	x_A (Expt)
	g/s	°C	°C	W/cm^2	W/cm^2		cm
Error	± 0.05	± 1	± 1	± 25%			± 12 %
1	0.702	56.6	48.6	0.18	0.19	4.1	71
2	0.700	56.6	49.8	0.16	0.14	13.4	90
3	0.700	56.6	50.0	0.15	0.13	11.5	93
4	0.698	56.6	50.7	0.12	0.11	4.2	95
5	1.000	57.0	44.0	0.40	0.40	0.6	57

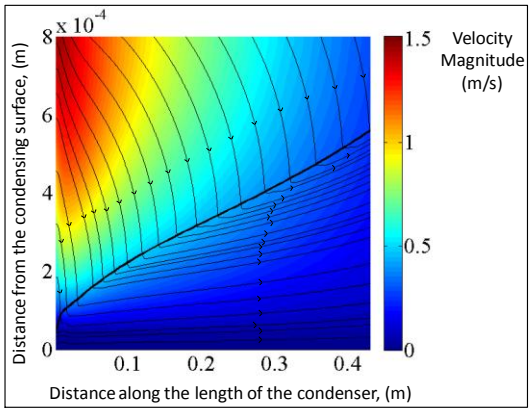

(a)

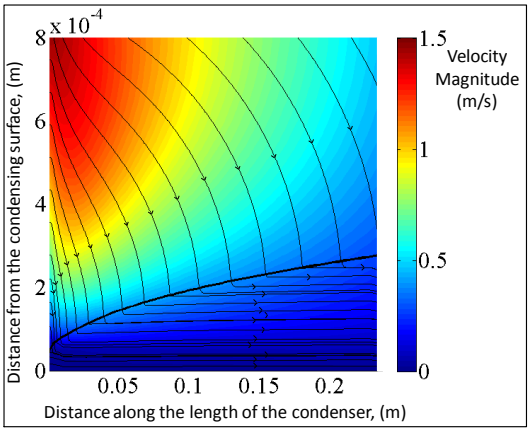

(b)

Figure 7. Streamline patterns of condensing flows in (a) shear-driven (b) 2 degree inclined gravity-assisted configurations showing differences in flow physics. (Fluid: FC- 72 vapor, $\dot{m}_{in}$ = 0.4 g/s, ΔT = 17.45 °C, and h = 2 mm)

5.4 Unsteady simulation results

Figure 8 shows a steady and unsteady simulation for an experimental case. The initial disturbance at t = 0 s (with three different wavelengths) and its unsteady evolution at t = 0.05 s are shown. The steepening and growing wave front around x = x_A has been assessed to indicate transition from annular to non-annular regimes. This is an on-going study and will be reported fully in a future publication.

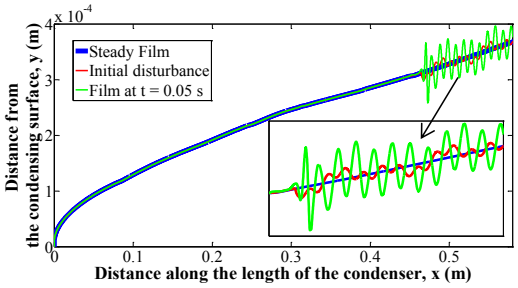

Figure 8. The 0 m ≤ x ≤ 0.57 m steady and unsteady simulations for an experimental case (fluid - FC-72, p_{in} = 101 kPa, h = 2 mm, $\dot{m}_{in}$ = 1.0 g/s, and experimental wall temperature variation).

6. Conclusions

• Fundamental 2-D steady/unsteady predictive tools for flow condensation have been developed. With regard to convergence and satisfaction of interfacial conditions in presence of waves, the tool shows excellent accuracy.

• The demonstrated compatibility of the scientific tool's predictions with the

experimentally obtained data further supports the validity of the tool and underlying model.

• Differences in physics between gravity driven and shear driven flows can be understood using these simulation tools.

• A path forward towards identifying the transition from annular to non-annular regimes has been proposed.

7. Acknowledgements

This work was supported by NSF Grant CBET-1033591.

8. References

1. Narain, A., et al., Results for Hight Heat-flux Realizations in Innovative Operations of Milli-meter Scale Condensers and Boilers, Proceedings of the 22th National and 11th International ISHMT-ASME Heat and Mass Transfer Conference, India, 2013

2. Narain, A., et al., Internal condensing flows inside a vertical pipe: Experimental/computational investigations of the effects of specified and unspecified (Free) conditions at exit. *Journal of Heat Transfer*, **129**, pp. 1352-1372, 2007

3. Kulkarni, S., A. Narain, and S. Mitra, Forced Flow of Vapor Condensing Over a Horizontal Plate (Problem of Cess and Koh): Steady and Unsteady Solutions of the Full 2D Problem. *Journal of Heat Transfer*, **132**, pp. 101502, 2010

4. Kurita, J., et al., Experimental results on gravity driven fully condensing flows in vertical tubes, their agreement with theory, and their differences with shear driven flows' boundary-condition sensitivities. *International Journal of Heat and Mass Transfer*, **54**, pp. 2932-2951, 2011

5. Phan, L. and A. Narain, Nonlinear stability of the classical Nusselt problem of film condensation and wave effects. *Journal of Applied Mechanics*, **74**, pp. 279-290, 2007

6. Narain, A., et al., Direct computational simulations for internal condensing flows and results on attainability/stability of steady solutions, their intrinsic waviness, and their noise sensitivity. *Journal of Applied Mechanics*, **71**, pp. 69-88, 2004

7. Mitra, S., R. Naik, and A. Narain, Numerical Simulation of Exact Two-Dimensional Governing Equations for Internal Condensing Flows, COMSOL Conference 2010, Boston, 2011

8. Mitra, S., Development Of One-Dimensional And Two-Dimensional Computational Tools To Simulate Steady Internal Condensing Flows In Terrestrial And Zero-Gravity Environments, Doctor of Philosophy, Mechanical Engineering, Michigan Technological University, 2012

9. Son, G. and V.K. Dhir, Numerical simulation of film boiling near critical pressures with a level set method. *Journal of Heat Transfer*, **120**, pp. 183-192, 1998

10. Mukherjee, A. and V.K. Dhir, Study of lateral merger of vapor during nucleate pool boiling. *Journal of Heat Transfer*, **126**, pp. 1023-1039, 2004

11. Sussman, M., P. Smereka, and S. Osher, A Level Set Approach for Computing Solutions to Incompressible 2-Phase Flow. *Journal of Computational Physics*, **114**, pp. 146-159, 1994

12. Osher, S. and R.P. Fedkiw, *Level set methods and dynamic implicit surfaces*. Applied mathematical sciences2003, New York: Springer. xii, 273 p.

13. Enright, D., et al., A hybrid particle level set method for improved interface capturing. *Journal of Computational Physics*, **183**, pp. 83-116, 2002

14. Gibou, F., et al., A level set based sharp interface method for the multiphase incompressible Navier-Stokes equations with phase change. *J. Comput. Phys.*, **222**, pp. 536-555, 2007

15. Mitra, S., et al., A quasi one-dimensional method and results for steady annular/stratified shear and gravity driven condensing flows. *International Journal of Heat and Mass Transfer*, **54**, pp. 3761-3776, 2011

16. Delhaye, J.M., Jump Conditions and Entropy Sources in Two-phase Systems; Local Instant Formulation. *International Journal of Multiphase Flow*, **1**, pp. 395-409, 1974

17. Kulkarni, S.D., et al., Condenser performance, Control, and Heat Transfer Enhancement Issues Resulting from Elliptic-Sensitivity of Shear Internal Condensing Flows. . *International Journal of Transport Phenomena*, **13**, pp. 15-57, 2012

18. Gorgitrattanagul, P., The length of the Annular Regime for Condesing Flows inisde a Horizontal Channel - The Experimental Determination of its Values and its Trends, Master of Science, Mechanical Engineering, Michigan Technological University, 2011